한국기계가공학회지, 제19권, 제7호, pp.81～88(2020.07) ISSN 1598-6721(Print)
Journal of the Korean Society of Manufacturing Process Engineers, Vol. 19, No. 7, pp.81~88(2020.07) ISSN 2288-0771(Online)

https://doi.org/10.14775/ksmpe.2020.19.07.081

Effects of Geometry and Imperfection of a Small-sized Groove on Stress Distributions in the Vicinity of the Joined Region of an ABS Part with a Thin Wall

Dong-Gyu Ahn*,#, Humayun Hassan*, Sun Ho Baek*, Ho Kim*

*Dept of Mechanical Engineering, Chosun Univ.

기저부에 생성된 작은 홈 형상과 결함이 박벽이 포함된 ABS 재료로 제작된 제품의 결합 영역 응력 분포에 미치는 영향

안동규*,#, 하산 후마윤*, 백선호*, 김 호*

*조선대학교 기계공학과

(Received 23 June 2020; received in revised form 01 July 2020; accepted 05 July 2020)

ABSTRACT

The geometry and the defect of the groove of the part provoke a sudden change of stress in a local region. The objective of this paper is to investigate the effects of the geometry and the imperfection of a small groove on stress distributions in the vicinity of the joined region for the ABS part with a thin wall using a three-dimensional finite element analysis (FEA). Several types of groove are designed to improve joining characteristics in the vicinity joined region. The imperfection model of the small-sized groove is obtained from observation of deposition characteristics of a fused deposition modeling process. Local stress distributions in the vicinity of the joined region are predicted by the FE model with refined meshes. The influence of the angle and the imperfection of the groove on appearance regions of the maximum stress and distributions of the defined principal stress for different loading conditions is examined using the results of FEAs. Finally, a proper design of the groove is proposed to improve joining characteristics between the substrate and the ABS part.

Keywords : Geometry(기하학적 형상), Imperfection(결함), Small-sized Groove(작은 크기의 홈), Joined Region (결합된 영역), Stress Distribution(응력 분포)

1. Introduction

Characteristic designs, such as protrusions, grooves, etc., in the vicinity of the joined region have been widely adopted to improve joining characteristics between dissimilar structures[1,2]. The groove type geometry has been used to increase joining strength between the substrate and the attached part through the contact area in the vicinity of the joined region[1-3]. The characteristic geometry of the groove greatly affects the joining strength between the

Corresponding Author : smart@chosun.ac.kr
Tel: +82-62-230-7043, Fax: +82-62-230-7234

substrate and the attached part. In addition, defects, including voids, porosity, cracks, etc. in the vicinity of the joined region significantly affect joining characteristics between dissimilar structures[4-6]. The geometry and the imperfection of the groove of the part provoke a sudden change of stress in a local region[7,8]. The formation of the groove can increase joining strength between the substrate and the deposited region by increasing the contact area[6,9].

Bürenhaus et al. have investigated that the influence of the groove design in the vicinity of the overlap joint on the adhesive bonding strength of the specimen through experiments[6]. They have fabricated the specimen using a fused deposition modeling (FDM) process. Kuznetsov et al. have investigated that the effects of the formation of the void in the fabricated part by a FDM process on the strength of the part via experiments[8]. Zareiyan et al. have examined the effects of the groove for interlocking on joining strengths of the specimen fabricated from a contour crafting process[9]. Sattari-Far et al. have studied that the influence of the groove shape on the residual stress distribution in butt-welded pipes through the repeated FEA[10]. Through the literature survey of previous research works, it has been noted that a small amount of research work is performed to examine the influence of the geometry of the groove and the imperfection of the substrate on the stress distribution in the vicinity of the joined region using finite element analyses (FEAs).

The objective of this paper is to investigate the effects of the geometry and the imperfection of a small-sized groove on stress distributions in the vicinity of the joined region for the ABS part with a thin wall using a three-dimensional FEA. Using the results of FEAs, proper designs of the groove of the substrate are proposed for different loading conditions. In addition, the effects of the imperfection of the groove on the stress distribution in the vicinity of the joined region are discussed.

2. Design of Analysis Model

2.1 Design of Model

Fig. 1 shows the geometry of the analysis model with the groove. The analysis model is extracted from the reference part created by the deposition of a thin wall on the substrate using a FDM process, as shown in Fig. 1(a). In order to minimize the effects of the end region on the stress distributions of the joined region, end regions of the reference part are removed in the analysis model. An acrylonitrile butadiene styrene copolymer (ABS) is chosen as the material of the thin wall and the substrate. The groove is assigned to a center region of the designed model, as shown in Figs. 1 (b) and (c). External dimensions of the analysis model are 50 mm × 40 mm × 20 mm.

The thickness of the thin wall and the depth of the groove are 3.0 mm and 0.2 mm, respectively.

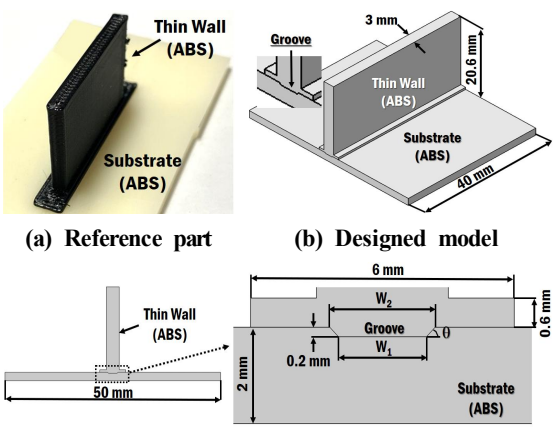

(a) Reference part (b) Designed model

(c) Characteristics dimensions

Fig. 1 Design of analysis model (w/o imperfection)

Table 1 Characteristic dimensions of groove for different groove angles (θ)

θ(°)	w/o. groove	w. groove			
		45	60	75	90
W_1	2.0				
W_2	-	2.3	2.2	2.1	2.0

Table 1 shows characteristic dimensions in the vicinity of the joined region for different groove angles (θ). The designed groove angle ranges from 45 ° to 90 °.

2.2 Design of Imperfection

A typical imperfection of the joined region for the reference part is obtained from the observation of the morphology in the vicinity of the groove for ABS deposited part on the ABS substrate using a FDM process, as shown in Fig. 2 (a). Through the observation of the morphology, it is noted that a dominant imperfection mode of the joined region is an insufficient filling of the deposited material in the groove. The deposited material is hardly filled in the small-sized groove when the insufficient filling is taken place. From these results, an insufficient filling with unfilled region is assumed to be a typical imperfection mode of the groove region. Using the estimated typical imperfection mode, a completely unfilled region is created in the analysis model with imperfection, as shown in Fig. 2 (b). All dimensions of the analysis model with imperfection are identical to those of the analysis model without imperfection.

3. Finite Element Analyses

FEAs are carried out using a commercial software ABAQUS V6.12. Fig. 3 shows mesh structures and

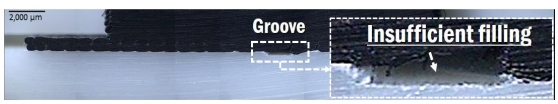

(a) Typical imperfection of the joined region

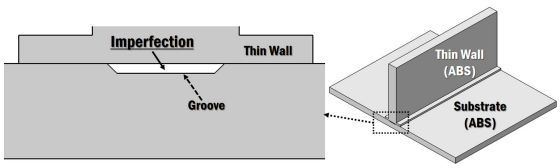

(b) Imperfection in the vicinity of the groove

Fig. 2 Design of analysis model with imperfection

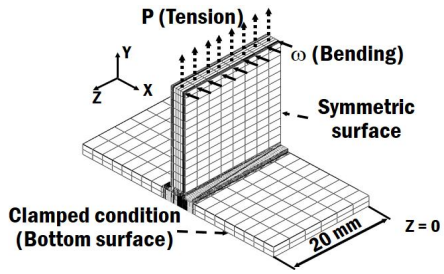

(a) Meshes and boundary conditions

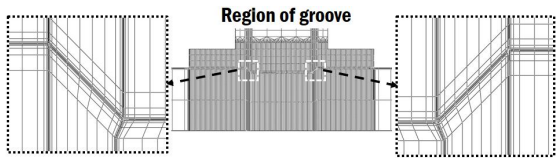

(b) Refined mesh structure (w/o imperfection)

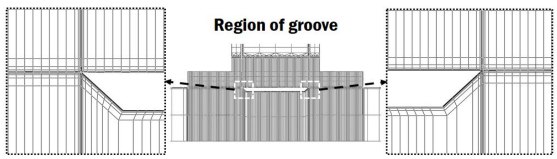

(c) Refined mesh structure (with imperfection)

Fig. 3 FE model and boundary conditions

Table 2 ABS properties and applied loads[11]

Elastic modulus (MPa)	Poisson's ratio	Density (g/mm^3)	P (N/mm^2)	ω (N/mm)
2,310	0.37	1.01×10^{-6}	0.1	0.045

boundary conditions of the FE model. In order to properly predict a local stress in the vicinity of suddenly changing region of geometry, the mesh refinement is applied to edge and conner regions using mapped and biased meshing techniques, as shown in Figs. 3 (b) and (c). Solid elements are used to represent the geometry of the model. The bottom surface of the FE model is fixed. A uniform tensile load (P) and a uniformly distributed load (ω) are applied to the top surface and the top edge of the thin wall for cases of tension and bending conditions, respectively. Table 2 shows material properties of ABS and the magnitude of the applied load.

Symmetric FE models are used to reduce analysis times, as shown in Fig. 3 (a).

4. Results and Discussion

4.1 Effects of the Groove Geometry

4.1.1 Tension

The effects of geometry of groove on the stress distribution in the vicinity of the joined region are investigated using results of FEAs for the analysis model without imperfection. The angle of the groove (θ) is chosen as the measure of variation of the groove geometry, as shown in Fig. 1 (c). The maximum value of maximum principal stress ($\sigma_{m,p}$) appears in the edge region of the thin wall irrespective of the angle of the groove for the case of the tensile loading, as shown in Fig. 4. In order to investigate the magnification of the localized stress according to the applied load, the normalized principal stress (σ_n) is defined, as Eq. (1).

$$\sigma_n = \sigma_{m,p}/P \tag{1}$$

Measured locations of the stress are indicated in Fig. 5 (a). The influence of the groove angle on normalized principal stress distributions is examined, as shown in Figs. 5 (b) and (c). A slight change of the normalized principal stress appears in the vicinity of coner of the groove, as shown in Fig. 5 (b). The maximum value of the normalized principal stress is

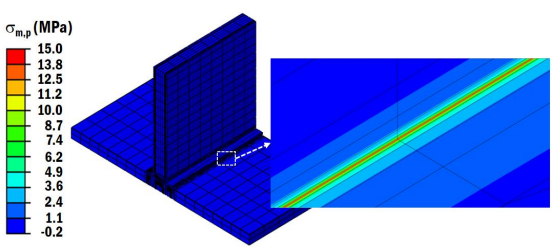

Fig. 4 Maximum principal stress ($\sigma_{m,p}$) distributions (Tensile load, θ = 45 º and w/o imperfection)

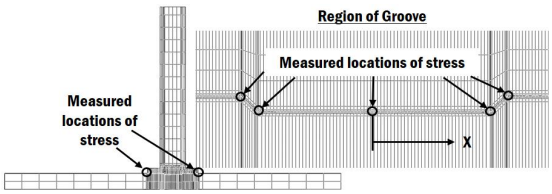

(a) Measured locations of stress

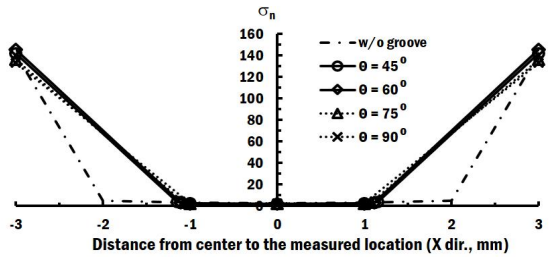

(b) σ_n distributions for different θs (Z = 0 mm)

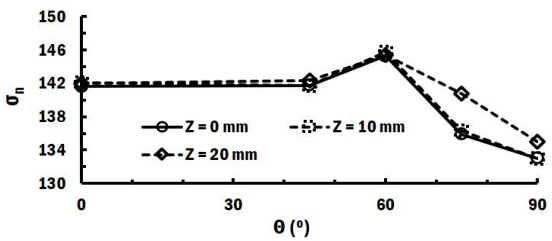

(c) Effects of θ on σ_n

Fig. 5 Influence of the groove angle on normalized principal stress distributions (Tensile load and w/o imperfection)

greater than 131 irrespective of the groove angle. The normalized principal stress increases when the groove angle changes from 45 º to 60 º, while that decreases when the groove angle increases from 60 º to 90 º, as shown in Fig. 5 (c). From these results, it is noted that a critical angle of the groove is 60 º when the tensile load is applied to the designed geometry.

4.1.2 Bending

The results of FEAs for the case of bending load shows that the maximum principal stress occurs at the edge of the load side regardless of the groove angle for the case of bending load, as shown in Fig. 6. The proportional principal stress for uniform bending

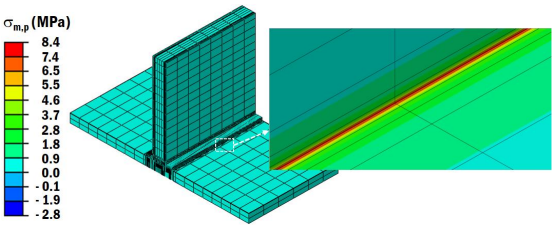

Fig. 6 Distributions of maximum principal stress (Bending load, θ = 45 ° and w/o imperfection)

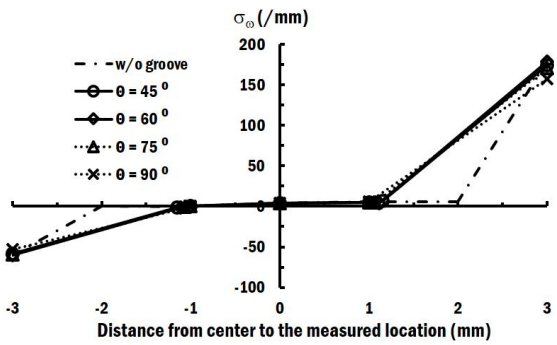

(a) σ_w distributions for different θs (Z = 0 mm)

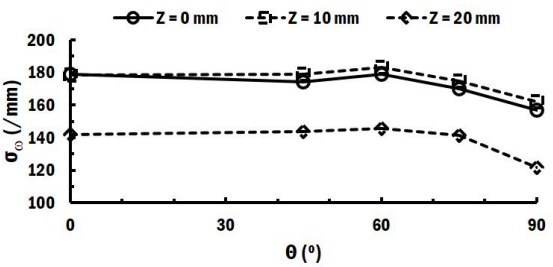

(b) Effects of θ on σ_w

Fig. 7 Influence of the groove angle on proportional principal stress distributions (Bending load and w/o imperfection)

load (σ_w) is defined to examine the amplification of the localized stress according to the applied bending load, as Eq. (2).

$$\sigma_w = \sigma_{m,p}/\omega \tag{2}$$

The effects of the groove angle on proportional principal stress distributions is investigated, as shown in Figs. 7 (a) and (b). The amplification of stress at conners of groove is almost negligible irrespective of the groove angle, as shown in Fig. 7 (a). A slight fluctuation of the stress appears in the sloped region of the groove for cases of 60 ° and 75 ° of the groove angle unlike 45 ° and 90 ° of the groove angle. The maximum value of the proportional principal stress ranges from 121 mm^{-1} to 179 mm^{-1}. The proportional principal stress slightly increases when the groove angle changes from 45 ° to 60 °, while that decreases when the groove angle increases from 60 ° to 90 °, as shown in Fig. 7 (b). From these results, it is revealed that a critical angle of the groove is 60 ° when the bending load is applied.

4.2 Effects of imperfection

4.2.1 Tension

The influence of the geometry and the imperfection of the groove on the stress distribution in the vicinity of the joined region is examined using results of FEAs for the analysis model with imperfection. The maximum value of the maximum principal stress is found in the edge region of the thin wall regardless of the groove angle for the case of the tensile loading, as shown in Fig. 8. The normalized principal stress of the edge region increases when the groove angle augments from 45 ° to 60 °, while that decreases when the groove angle increases from 60 ° to 90 °, as shown in Fig. 9 (a). These results are

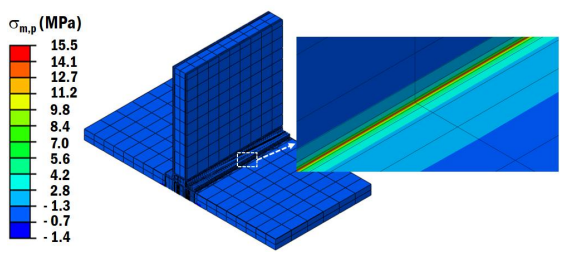

Fig. 8 Distributions of maximum principal stress (Tensile load, θ = 60 ° and imperfection)

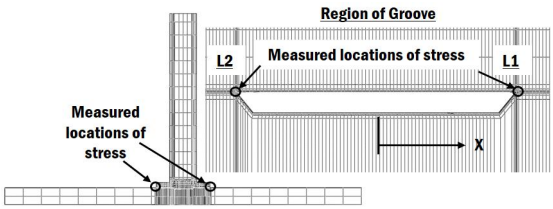

(a) Measured locations of stress

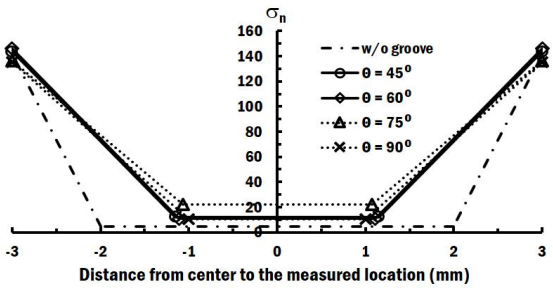

(b) σ_n distributions for different θs (Z = 0 mm)

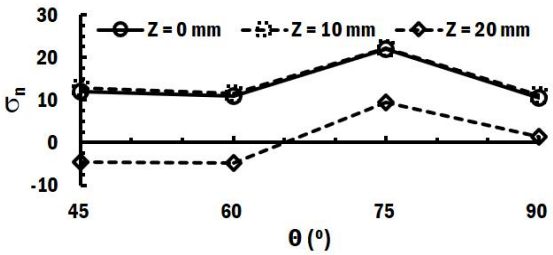

(c) Effects of θ on σ_n (Measured location = L1)

Fig. 9 Influence of the groove angle on normalized principal stress distributions (Tensile load and imperfection)

almost similar to those for the analysis model without imperfection for the case of the tensile loading. The maximum value of the maximum principal stress for the analysis model with imperfection is identical to that for the analysis model without imperfection irrespective of the groove angle.

The variation of the normalized principal stress according to the groove angle in corner regions of the groove, which are L1 and L2 in Fig. 9 (a), is somewhat different from that in edge regions of the thin wall, as shown in Fig. 9 (c). The normalized principal stress in the region of L1 is maximized when the groove angle is 75 °. The normalized principal stress in the L1 region is nearly 16 % of that in the edge region when the groove angle is 75 °. However, normalized principal stresses in the L1 region are less than 10 % of those in the edge region when groove angles are 45 °, 60 ° and 90 °. From these results, it is revealed that the critical angle of the groove is 75 ° from the viewpoint of the normalized principal stress of the L1 region for the case of tensile loading when the imperfection is taken place in the groove.

4.2.2 Bending

The results of FEAs with imperfection for the case of bending load shows that the maximum principal stress taken place at the conner region of the groove in the opposite side of the applied region of the load (L2) irrespective of the groove angle for the case of bending load, as shown in Fig. 10. The coner region, at which the maximum principal stress appears, is located at the end of the model in the Z direction, as shown in Figs. 10, 11 (a) and 11 (b).

The proportional principal stress of the edge region of the thin wall is less than 194 mm^{-1} irrespective of the groove angle when the imperfection is taken place in the groove. The proportional principal stress at the location of L2 exceeds the maximum value of the proportional principal stress of the edge region when the groove angle is 60 ° and 75 °, while that is less than the maximum value of the proportional principal

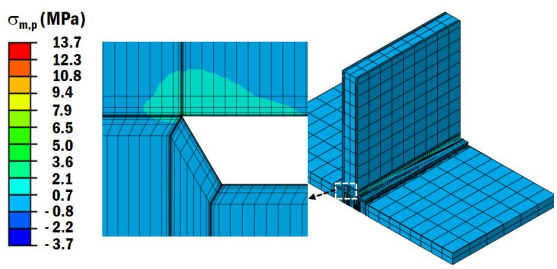

Fig. 10 Distributions of maximum principal stress (Tensile load, imperfection, θ = 60 °)

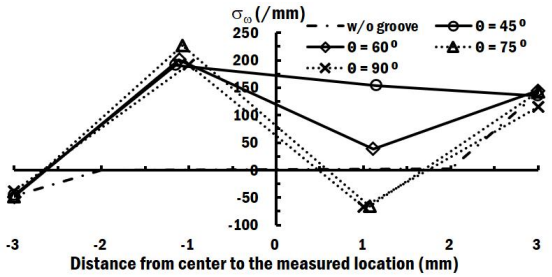

(a) σ_w distributions for different θs (Z = 20 mm)

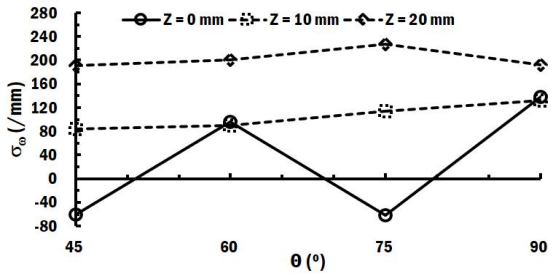

(b) Effects of θ on σ_w (Measured location = L2)

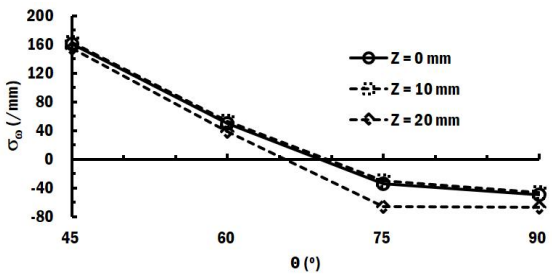

(c) Effects of θ on σ_w (Measured location = L1)

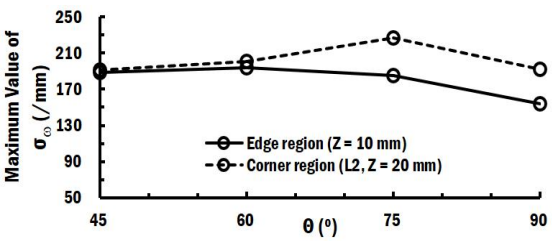

(d) Maximum value of σ_w for different regions

Fig. 11 Influence of the groove angle on proportional principal stress distributions (Bending load and imperfection)

stress of the edge region when the groove angle is 45 ° and 90 °. The proportional principal stress at the coner region of the groove in the applied region of the load (L1) decreases when the groove angle increases, as shown in Fig. 11 (c).

4.3 Proper design of groove

Through the investigation of the results of FEAs for the analysis model without imperfection, it is shown that the amplification of stress is maximized when the groove angel is 60 °. In addition, it is revealed that the fluctuation of the stress takes place in the sloped region of the groove when the groove angle is 60 ° and 75 °, while the smooth transition of stress in the sloped region of the groove when the groove angle is 45 °. From the results of FEAs for the analysis model with imperfection, it is revealed that the critical location, at which the maximum stress appears, changes from the edge region of the thin wall to the corner region of groove in the vicinity of the end of the model when the loading condition is varied from tension to bending. The maximum value of the proportional principal stress at the coner region of the groove is less than that of the edge region of the thin wall irrespective of loading condition when the groove angle is 45 ° and 90 °, as shown in Fig. 11 (d). Considering the improvement of flow characteristics of ABS plastic into the groove, it is desirable to reduce the angle of the groove. Based on above results, the geometry with 45 ° of the groove angle is decided to a proper design of the small-sized groove.

5. Conclusion

The effects of the geometry and the imperfection of a small-sized groove on stress distributions in the vicinity of the joined region for the ABS part with a thin wall were investigated using a three-dimensional FEA. Various FE models, including the small-sized groove and the imperfection, were contrived to perform FEAs. Several types of groove, including

different groove angles, were designed.

From the results of FEAs for the analysis model without imperfection, it was shown that the maximum stress appears in the vicinity of the edge of the thin wall irrespective of the loading condition and the groove angle. The amplification of stress was maximized when the groove angel was 60 °. A smooth transition of stress in the sloped region of the groove appeared when the groove angle was 45 °.

From the results of FEAs with imperfection, it was shown that a critical location, at which the maximum stress occurs, varies from the edge region of the thin wall to the corner region of groove in the vicinity of the end of the model when the loading condition changes from tension to bending. The maximum stress at the critical location was less than that of the edge region of the thin wall irrespective of loading condition when the groove angle was 45 °.

Considering the results of FEAs and the flow characteristics of ABS plastic into the groove, the geometry with 45 ° of the groove angle was proposed to an appropriate design of the small-sized groove.

In the future, additional FE analyses and experiment should be performed to obtain the desired FE model with the improved accuracy and the optimum groove design with the enhanced safety and flow characteristics.

References

1. Weddeling, C., Woodward, S. T., Marrè, M., Nellesen, J., Psyk, V., Tekkaya, A. E., and Tillmann, W., “Influence of Groove Characteristics on Strength of Form-fit Joints,” Journal of Materials Processing Technology, Vol. 211, Issue. 5, pp. 925-935, 2011.
2. Tu, W., Wen, P. H., Hogg, P. J., and Guild, F. J., “Optimisation of the Protrusion Geometry in Comeld™ Joints,” Composites Science and Technology, Vol. 71, Issue. 6, pp. 868-876, 2011.
3. Aripin, M. A., Sajuri, Z., Abdullah, S., Omar, M. Z., Zmari, W. F. H., Jamil, W. N. M., and Abdullah, M. F., “Microscale Groove Effect on Shear Strength of Epoxy-bonded Dissimilar Metal Plate,” Journal of Adhesion Science and Technology, Vol. 30, No. 18, pp. 2001-2012,
4. Gebisa, A. W., and Lemu, H. G., “Investigating Effects of Fused-Deposition Modeling (FDM) Processing Parameters on Flexural Properties of ULTEM 9085 Using Designed Experiment,” Materials, Vol. 11, No. 4, pp. 500-522, 2018.
5. Kumar, R., Singh, R., and Ahuja, I. P. S., “Mechanical, Thermal and Micrographic Investigations of Friction Stir Welded: 3D Printed Melt Flow Compatible Dissimilar Thermoplastics,” Journal of Manufacturing Processes, Vol. 38, pp. 387-395, 2019.
6. Bürenhaus, F., Moritzer, E., and Hirsh, A., “Adhesive Bonding of FDM-manufactured Parts Made of ULTEM 9085 Considering Surface Treatment, Surface Structure, and Joint Design,” Welding in the World, Vol. 38, Issue. 6, pp. 1819-1832, 2019.
7. Chen, K. -S., Yeh, H. -M., Yan, J. -L., and Chen, Y. -T., “Finite-element Analysis on Wafer-level CMP Contact Stress: Reinvestigated Issues and the Effects of Selected Process Parameters,” International Journal of Advanced Manufacturing Technology, Vol. 42, Issue. 11-12, pp. 1118-1130, 2009.
8. Kuznetsov, V. E., Solonin, A. N., Tavitov, A., Urzhumtsev, O., and Vakulik, A., “Increasing Strength of FFF Three-dimensional Printed Parts by Influencing on Temperature-related Parameters of the Process,” Rapid Prototyping Journal, Vol. 26, No. 1, pp. 107-121, 2020.
9. Zareiyan, B., and Khoshnevis, B., “Effects of Interlocking on Interlayer Adhesion and Strength of Structures in 3D Printing of Concrete,” Automation in Construction, Vol. 83, pp. 212-221, 2017.
10. Sattari-Far, I., and Farahani, M. R., “Effect of the Weld Groove Shape and Pass Number on Residual Stresses in Butt-welded Pipes,” International Journal of Pressure Vessels and Piping, Vol. 86, Issue 11, pp. 723-731, 2009.
11. Beanumont, “Moldflow Material Characterization,” https://www.beaumontinc.com/moldflow-material-characterization/, accessed by 2020.